Journal of Plant Research (2018) 131:789–802
https://doi.org/10.1007/s10265-018-1049-2

REGULAR PAPER

Low assimilation efficiency of photorespiratory ammonia in conifer leaves

Shin-Ichi Miyazawa[1] · Mitsuru Nishiguchi[1] · Norihiro Futamura[1] · Tomohisa Yukawa[2] · Mitsue Miyao[3] · Tsuyoshi Emilio Maruyama[1] · Takayuki Kawahara[4]

Received: 5 April 2018 / Accepted: 28 May 2018 / Published online: 9 June 2018

Abstract

Glutamine synthetase (GS) localized in the chloroplasts, GS2, is a key enzyme in the assimilation of ammonia (NH_3) produced from the photorespiration pathway in angiosperms, but it is absent from some coniferous species belonging to Pinaceae such as *Pinus*. We examined whether the absence of GS2 is common in conifers (Pinidae) and also addressed the question of whether assimilation efficiency of photorespiratory NH_3 differs between conifers that may potentially lack GS2 and angiosperms. Search of the expressed sequence tag database of *Cryptomeria japonica*, a conifer in Cupressaceae, and immunoblotting analyses of leaf GS proteins of 13 species from all family members in Pinidae revealed that all tested conifers exhibited only GS1 isoforms. We compared leaf NH_3 compensation point (γ_{NH3}) and the increments in leaf ammonium content per unit photorespiratory activity (NH_3 leakiness), i.e. inverse measures of the assimilation efficiency, between conifers (*C. japonica* and *Pinus densiflora*) and angiosperms (*Phaseolus vulgaris* and two *Populus* species). Both γ_{NH3} and NH_3 leakiness were higher in the two conifers than in the three angiosperms tested. Thus, we concluded that the absence of GS2 is common in conifers, and assimilation efficiency of photorespiratory NH_3 is intrinsically lower in conifer leaves than in angiosperm leaves. These results imply that acquisition of GS2 in land plants is an adaptive mechanism for efficient NH_3 assimilation under photorespiratory environments.

Keywords Ammonia · Angiosperm · Chloroplastic glutamine synthetase (GS2) · Conifer · NH_3 compensation point · Photorespiration

Introduction

Glutamine synthetase (GS) is a key enzyme of ammonia (NH_3) assimilation and catalyzes the following reaction (Lea et al. 1990):

$$\text{Glutamate} + NH_3 + \text{ATP} \xrightarrow{Mg^{2+}} \text{Glutamine} + \text{ADP} + \text{Pi}.$$

There are two major isoforms of GS: cytosolic (GS1) and chloroplastic (GS2) forms. The molecular mass of GS1 ranges from 39 to 40 kDa, whereas that of GS2 can be as large as 42 kDa in French bean (*Phaseolus vulgaris* L.) and hybrid poplar (*Populus tremula* x *Populus alba*) (Castro-Rodríguez et al. 2011; Lightfoot et al. 1988). The GS2 gene of bean has a sequence for long N-terminal extension that acts as a chloroplast targeting sequence (Lea 1997; Lightfoot et al. 1988). In general, GS1 is involved in nitrogen translocation from leaves (Bauer et al. 1997; Kamachi et al. 1992) and lignin synthesis (Razal et al. 1996; Sakurai et al.

Electronic supplementary material The online version of this article (https://doi.org/10.1007/s10265-018-1049-2) contains supplementary material, which is available to authorized users.

✉ Shin-Ichi Miyazawa
miyashin@ffpri.affrc.go.jp

[1] Department of Forest Molecular Genetics and Biotechnology, Forestry and Forest Products Research Institute (FFPRI), 1 Matsunosato, Tsukuba 305-8687, Japan

[2] Tsukuba Botanical Garden, National Museum of Nature and Science, 4-1-1 Amakubo, Tsukuba 305-0005, Japan

[3] Graduate School of Agricultural Science, Tohoku University, Aoba, Sendai 980-0845, Japan

[4] Hokkaido Research Center, FFPRI, 7 Hitsujigaoka, Toyohira, Sapporo, Hokkaido 062-8516, Japan

1996), etc. whereas GS2 is involved in photorespiration in angiosperms (Somerville and Ogren 1980; Wallsgrove et al. 1987).

Photorespiration starts with the oxygenation of ribulose-1,5-bisphosphate (RuBP) by Rubisco. Two molecules of the oxygenation product, 2-phosphoglycolate (2-PG), are converted to the Calvin cycle intermediate 3-phosphoglycerate (3-PGA) by metabolism that involves release and re-assimilation of NH_3 by GS2. GS2-deficient barley mutants show a dramatic decline of the net CO_2-fixation rate and eventually necrosis after transfer from a non-photorespiratory (1% O_2) to a photorespiratory condition (ambient O_2 level of approximately 20%) (Blackwell et al. 1987; Wallsgrove et al. 1987). Transgenic tobacco plants overexpressing GS2 increase a tolerance to while those reducing GS2 are severely damaged to high light intensity where active photorespiration occurs (Kozaki and Takeba 1996). These results strongly support that GS2 is an essential enzyme for angiosperm photorespiration.

In contrast to angiosperm species, a conifer, *Pinus sylvestris*, possesses two cytosolic GS isoforms, GS1a and GS1b, but lacks GS2 (Avila et al. 1998; Cantón et al. 1993). Immunohistochemical analyses of *P. sylvestris* seedling have shown that GS1a localizes in chloroplast-containing tissues such as cotyledons whereas GS1b localizes in vascular tissues, suggesting an involvement of GS1a with photorespiratory NH_3 assimilation (Avila et al. 2001; Suárez et al. 2002).

A phylogenetic analysis of GS genes from prokaryotes, green algae and land plants including 10 angiosperms and *P. sylvestris* demonstrated that GS2 evolved from a duplicated GS1 gene rather than the gene transferred from the plastid endosymbiont genome (Avila-Sáez et al. 2000). Based on this phylogenetic analysis, Cánovas et al. (2007) speculated that acquisition of GS2 is an adaptive mechanism to high levels of photorespiratory NH_3 when plants encountered the present oxygen levels in the atmosphere during land plant evolution. However, there is no physiological evidence to support this hypothesis so far.

Assimilation efficiency of NH_3 during photorespiration in vivo can be evaluated on the basis of leaf NH_3 gas exchange. NH_3 in the mesophyll cells—its amount partly reflects the balance between NH_3 assimilation activity by leaf GS and NH_3 production activity by photorespiration—diffuses out from the apoplastic surface of the mesophyll cells through stomata to the ambient air when air-NH_3 concentration is low (Farquhar et al. 1980a; Kumagai et al. 2011; Miyazawa et al. 2014). Leaf NH_3 gas exchange has been intensively studied in crops and grasses. By contrast, NH_3 gas exchange studies are rarely reported in conifers.

The absence of GS2 from some other conifers in the family Pinaceae such as *Pinus pinaster, Pinus pinea, Abies pinsapo*, and *Larix decidua* have been confirmed by immunoblotting (Cánovas et al. 1991; García-Gutiérrez et al. 1998). It remains obscure whether GS2 is present or absent in conifers from the other five family members in Pinidae (Araucariaceae, Cupressaceae, Podocarpaceae, Sciadopityaceae, and Taxaceae).

Here we examined the absence of GS2 in leaves of coniferous species from all the family members. In particular, *Cryptomeria japonica* D.Don, "Sugi" in Japanese—a coniferous species that belongs to the family Cupressaceae—is crucial to the forestry and wood industries of Japan. More than 50,000 expressed sequence tags (ESTs) are available in the sugi database (ForestGEN). We utilized the EST database of sugi to search for the GS orthologues. We also addressed the question of whether that assimilation efficiency of photorespiratory NH_3 was lower in conifers that may potentially lack GS2 than in angiosperms through leaf NH_3 gas exchange.

Materials and methods

Plant materials for NH_3 gas exchange, GS activity and NH_3 leakiness measurements

GC-grown plants

We grew *C. japonica* (sugi), *Phaseolus vulgaris* L. cv. "Kentucky" (French bean), and *Populus nigra* L. (black poplar) plants in an environmentally controlled growth chamber (GC, Koito Electric Industries Ltd.; Yokohama, Japan). Bean plants were grown from seeds, and black poplar and sugi plants were propagated from cuttings. Bean and poplar plants were grown in Wagner pots (113 mm in internal diameter, 1.4-l in volume) filled with vermiculite. Sugi plants were cultured in the pots filled with a mixture (1:1 by volume) of Kanuma pumice and red granular soils.

Bean and black poplar plants were cultured in the GC under the photosynthetically active photon flux density (PPFD) of 400 μmol m^{-2} s^{-1}. This PPFD, however, induces a yellowing symptom in sugi leaves. Therefore, sugi plants were cultured in a separate GC under the low PPFD of 170 μmol m^{-2} s^{-1}. Day/night air temperature and relative humidity were set at 25/20 °C and 70%, respectively. Day/night periods were set at 16 h/8 h.

Potted plants were placed in the stainless-steel containers of a custom-made automatic water-supplying system. The containers had a maximum load of 20 Wagner pots. The system for bean and black poplar plants was equipped with a 60-l tank of nutrient solution, which comprised 1.8 mM NH_4NO_3, 0.35 mM NaH_2PO_4, 0.63 mM KCl, 0.36 mM $CaCl_2$, 0.25 mM $MgSO_4$, 0.06 mM H_3BO_3, 0.06 mM Fe(III)-EDTA, 0.4 μM Cu(II)-EDTA, 0.4 μM Mn(II)-EDTA, and 0.3 μM Zn(II)-EDTA. The system for sugi was supplied with the same nutrient composition at half strength. The bottoms

of bean and black poplar pots were automatically soaked in nutrient solution for 15 min twice a day and those of sugi pots were soaked in nutrient solution three times a week. The nutrient solution was renewed every 2 weeks.

As described above, the sugi plants were grown under the different growth condition (low- light and low-nutrient supply, "L-condition") from the condition where the bean and black plants were grown (high-light and high-nutrient supply, "H-condition"). We also raised black poplar plants grown under the L-condition for measurements (namely, the same conditions including soil type, PPFD and levels of nutrient supply as for sugi).

Black poplar and sugi plants had heights of 50–70 cm and 30–50 cm, respectively. We used bean plants of which the first trifoliate leaves had been just emerged. Mature leaves from the upper parts of black poplar and sugi shoots and primary leaves from bean plants were used for all experiments. Leaves were sampled from at least three plants.

Field-grown plants

Adult trees of *Pinus densiflora* Siebold & Zucc. (pine), *Populus alba* L. (silver poplar), and sugi grown in the FFPRI tree garden (Tsukuba, Japan) under field conditions were used for experiments; the sunlit branches of two to three individuals of each species were used during the periods of June to early September in 2015 or 2016. Diameters at breast height of the pine, silver poplar, and sugi trees were 37–53 cm, 33–64 cm, and 10–12 cm, respectively. We designated those samples as field-condition ("F-condition") samples.

Plant materials for immunoblotting analysis

We collected current-year mature leaves of adult pine, silver poplar and sugi trees for immunoblotting analysis. We also collected current-year mature leaves of other coniferous species including *Cedrus deodara* (Roxb. ex D.Don) G.Don, *Cephalotaxus harringtonia* (Knight ex J.Forbes) K.Koch, *Chamaecyparis obtusa* Siebold & Zucc., *Juniperus rigida* Wall. ex Carrière, *Larix kaempferi* Fortune ex Gordon, *Metasequoia glyptostroboides* Hu & W.C.Cheng, *Podocarpus macrophyllus* D.Don, *Sciadopitys verticillata* Siebold & Zucc., *Taxus cuspidata* Siebold & Zucc., and *Thuja standishii* Carrière. We also collected current-year mature leaves of angiosperm species including *Fagus crenata* Blume, *Firmiana simplex* W.Wight, *Illicium anisatum* Bartr. ex Michx., *Magnolia praecocissima* Koidz., and *Morus australis* Poir. and collected mature leaves of a gymnosperm, *Ginkgo biloba* L. All of these species were cultivated in the FFPRI tree garden (Tsukuba, Japan) and were sampled during early September 2015.

Leaves of *Cycas revoluta* Thunb., *Ephedra minima* K.S.Hao, *Gnetum gnemon* L., *Welwitschia mirabilis* Hook.f. were collected in June 2016 and current-year leaves of *Araucaria angustifolia* (Bertol.) Kuntze and *Wollemia nobilis* W.G.Jones, K.D.Hill & J.M.Allen were collected in November 2016 in Tsukuba Botanical Garden (Tsukuba). We also collected samples of the GC-grown plants: mature primary leaves and roots of bean, current-year shoots of sugi, mature leaves of black poplar, and rosette leaves of *Arabidopsis thaliana* (L.) Heynh. Those samples were immediately frozen in liquid N_2 and stored in a freezer at − 80 °C until use.

Phylogenetic tree

We retrieved the deduced amino acid sequences of *GS* genes of French bean, *Populus trichocarpa*, and *Pinus sylvestris* from the database of the National Center for Biotechnology Information (NCBI; http://www.ncbi.nlm.nih.gov/). The Arabidopsis *GS* sequence was used as a query to search for orthologues of sugi *GS* in the EST database (ForestGEN; http://foresgen.ffpri.affrc.go.jp/en/info_cj.html). Two *GS* orthologues were found and were designated as *CjGS1a* and *CjGS1b*. A phylogenetic tree based on alignments of the deduced full-length amino acid sequences of *GS* genes (Fig. S1) was constructed with the neighbor-joining method using software (MEGA 6.0; Tamura et al. 2013). The number of bootstrap replicates was set at 1000. Molecular masses of sugi GS were predicted using ExPASy (http://web.expasy.org/compute_pi/). The amino acid positions of the cleavage sites for the GS2 transit peptides were predicted using ChloroP (http://www.cbs.dtu.dk/services/ChloroP/).

Immunoblotting

Soluble protein was extracted from leaf samples (root samples as well for French bean) in accordance with the method described by Tsuchida et al. (2001) using a slightly modified formulation of their reported extraction buffer. Specifically, our extraction buffer contained 50 mM HEPES-KOH (pH 7.8), 1 mM EDTA, 10% (v/v) glycerol, 10 mM $MgSO_4$, 5 mM DTT, 0.01 mM leupeptin, and 1% (v/v) nonidet P-40.

Immunoblotting analysis was performed using a semi-dry system in accordance with the manufacturer's protocol (Bio-Rad, Hercules, CA, USA). Four micrograms of the soluble proteins were subjected to SDS–PAGE per lane. Proteins separated through SDS–PAGE were transferred to a nitrocellulose membrane. GS polypeptides were reacted with anti-GS1 GS2 global antibody (Agrisera AB, Vannas, Sweden) then with a goat-rabbit antibody for alkaline phosphatase detection. Soluble protein content was determined by Bradford method (Bradford ULTRA; Expedeon, San Diego, CA).

Photosynthesis

Photosynthetic parameters were measured using a portable CO_2/H_2O gas exchange analyzer (LI-6400; LI-COR, Lincoln, NE, USA) equipped with a cylindrical transparent chamber (Model 6400-05). The parameters include net CO_2 fixation (A) and transpiration (E) rates, stomatal conductance to water vapor (g_s), the total conductance to water vapor (g_{tot}, the conductance to water vapor through stomata and the boundary layer surrounding the leaf), and CO_2 concentration of intercellular air apace (C_i). Light was provided by a tungsten–halogen light source (LS2; Hansatech, King's Lynn, UK). Incident PPFD on the leaves was 800 µmol m^{-2} s^{-1} (an approx. light-saturated level of A for studied plants). Flow rate entering the chamber (u_e) and chamber air temperature were set at 700–750 µmol s^{-1} and 25 °C, respectively. Leaf-to-air vapor pressure deficit in the chamber ranged from 0.5 to 2.2 kPa. Leaf boundary layer conductance to water vapor for two-sided surfaces (g_{bw}) was estimated through the filter paper method in reference to the LI-6400 manual and ranged from 1.5 to 2.0 mol m^{-2} s^{-1} for bean and black and silver poplars. The g_{bw} of sugi and pine were set at 8 mol m^{-2} s^{-1}, a default value of LI-6400. Leaf temperature calculated through the energy budget method of the LI-6400 program was 25–27 °C.

NH_3 gas exchange and NH_3 compensation point (γ_{NH3})

Leaf NH_3 absorption rate (F_{NH3}) linearly increases with increasing atmospheric NH_3 concentration surrounding the leaf (n_a). F_{NH3} is written as follows (Farquhar et al. 1980a):

$$F_{NH3} = g_{NH3}\left(n_a - \gamma_{NH3}\right), \quad (1)$$

where g_{NH3} and γ_{NH3} are the total conductance to NH_3 diffusion and the NH_3 compensation point, respectively. Leaves emit NH_3 to the atmosphere when n_a is lower than γ_{NH3} (Farquhar et al. 1980a).

We simultaneously measured F_{NH3} and CO_2/H_2O gas exchange rates. The air-inlet port of LI-6400 was connected to an NH_3-absorbing column, which removed NH_3 from the air supplied by a gas cylinder (20% O_2 balanced in N_2). The column contained 500 g of 5 mm diameter glass beads, which had been previously smeared with 5% (v/v) phosphoric acid and 2% (v/v) glycerol and dried overnight at 60 °C. A dew-point generator (LI-610; LI-COR) was connected between the column and cylinders to humidify the cylinder air. The outlet port, which vented air from the LI-6400 chamber, was linked to a chemiluminescence NH_3 analyzer (ML9841A; Teledyne Monitor Labs, Englewood, CO, USA). All devices were connected using polytetrafluoroethylene tubing. A vent tube located between the devices was used to prevent air pressure from increasing in the analyzers. F_{NH3} was determined using a following equation (Miyazawa et al. 2014).

$$F_{NH3} = \left(n_e - n_o\right)u_e/\mathrm{LA} - n_oE, \quad (2)$$

where n_o is the mole fraction of NH_3 in the air leaving the chamber when the chamber contains leaves. Changes in air-NH_3 concentration with time were logged. n_e, the NH_3 mole fraction of air without leaves, was estimated from baseline values. After measurements, we took digital photographs of the leaves in the portable gas exchange chamber to estimate projected leaf area (LA) from the photographs using Image J (1.48v; NIH, Bethesda, MD, USA).

The γ_{NH3} was determined with Eq. 1. Theoretically, g_{NH3} equals 0.92 times the g_{tot} (Farquhar et al. 1980a). n_a was assumed equal to n_o. Leaf temperatures for NH_3 gas exchange measurements were similar to those described above. The CO_2 concentration in the portable gas exchange chamber was set at ambient level (400 ppm) throughout the measurements.

NH_3 leakiness

For NH_3 leakiness experiments, GC-grown plants were transferred to the laboratory before GC-light bulbs were turned on. Branches of field-grown plants were transferred to the laboratory on the evening 1 day before measurement dates. When sampling the branches, stem ends were cut in tap water to prevent air embolism. Illuminated leaves inside the LI-6400 chamber were subjected to different CO_2 levels (100–800 ppm) for an hour. The steady-state values of A and C_i were obtained. For dark treatment, the chamber was covered with black clothes to make leaves inside the chamber in dark under ambient CO_2 level (400 ppm) for an hour.

Leaves subjected to CO_2 or dark treatments were cut while still in the chamber, immediately frozen in liquid N_2, weighed and stored at − 80 °C. Leaf ammonium (NH_4^+) was extracted using 20 mM formic acid (Husted et al. 2000). NH_4^+ content was determined fluorometrically using HPLC after reaction with o-phthalaldehyde (474 Scanning Fluorescence Detector; Nihon Waters, Tokyo). We defined NH_3 leakiness as:

$$\mathrm{NH_3\ leakiness} = \frac{[\mathrm{NH_4^+}]^{100} - [\mathrm{NH_4^+}]^{800}}{v_o^{100} - v_o^{800}} \times \frac{1}{t}, \quad (3)$$

where $[NH_4^+]$, v_o, and t were leaf NH_4^+ content, Rubisco oxygenation rate, and CO_2 treatment period, respectively. t was 3600s. The superscript number (100 or 800) indicates CO_2 concentration (ppm) for CO_2 treatment. For each tested plant, we used the mean value of NH_4^+ content and that of v_o at respective CO_2 treatments for the calculations.

We did not measure LA of the leaf samples using a digital camera for NH_3 leakiness measurements because taking clear photographs needs turning off the light projected on the leaves thereby possibly interrupts correct determination of the leaf NH_4^+. Therefore, the gas exchange parameters including v_o were expressed per unit chlorophyll content. Leaf chlorophyll content per fresh weight was determined spectrophotometrically after pigment extraction with 80% (v/v) acetone (Porra et al. 1989). Chlorophyll contents per unit projected leaf area were determined using different leaf samples.

Rubisco oxygenation rate (v_o)

Rubisco oxygenation rate (v_o) was determined from leaf photosynthesis parameters with the FvCB model (Farquhar et al. 1980b):

$$v_o = 2\Gamma^*\left(A + R_{\text{day}}\right)/\left(C_c - \Gamma^*\right), \tag{4}$$

and

$$\Gamma^* = 0.5O_c/S_{\text{c/o}}, \tag{5}$$

where R_{day} is day respiration rate, C_c and O_c are CO_2 and O_2 concentrations in chloroplasts, respectively, and $S_{\text{c/o}}$ is the relative specificity factor of Rubisco. R_{day} was assumed to equal the steady-state rate of respiration in the dark (R_{dark}) (Epron et al. 1995). The $S_{\text{c/o}}$ of bean plants was obtained from the literature (Hermida-Carrera et al. 2016). Given that the $S_{\text{c/o}}$ values of poplar, sugi, and pine trees are unknown, tobacco $S_{\text{c/o}}$ values at a specific leaf temperature were used for these plants (Bernacchi et al. 2002). Under ambient O_2 level (20% O_2), calculated Γ* values (μmol mol^{-1}) at a measured leaf temperature for Bean_H, BPop_L, BPop_H, and Sugi_L were 40 at 26 °C, 39 at 26 °C, 37 at 25 °C, and 40 at 27 °C, respectively; those of SPop_F, Sugi_F and Pine_F were all 40 at 27 °C (see Table 1 for these abbreviations). C_c was calculated as:

$$C_c = C_i - A/g_m, \tag{6}$$

where g_m is mesophyll conductance to CO_2 gas diffusion.

Mesophyll conductance (g_m)

To determine g_m by the curve-fitting method (Ethier and Livingston 2004), A–C_i curves were separately obtained from CO_2 and dark treatment experiments (Fig. S2). For low C_i portions (< 220 ppm), the relationship of A against C_i is given as

$$\begin{aligned} A &= \frac{-b + \sqrt{b^2 - 4ac}}{2a} \\ a &= -1/g_m \\ b &= (V_{\text{cmax}} - R_{\text{day}})/g_m + C_i + K_c^{\text{air}} \\ c &= R_{\text{day}}(C_i + K_c^{\text{air}}) - V_{\text{cmax}}\left(C_i - \Gamma^*\right), \end{aligned} \tag{7}$$

where V_{cmax} and K_c^{air} are the maximum Rubisco carboxylation rate and the Michaelis–Menten constants of Rubisco for CO_2 under ambient O_2, respectively. The curve-fitting procedure was performed with nonlinear least-squares fits (Levenberg–Marquardt algorithm) using software (Origin 9.1J; Origin Lab., Northampton, MA, USA). Bean K_c^{air} was taken from the literature (Hermida-Carrera et al. 2016). Tobacco K_c^{air} values at a respective leaf temperature were used as the K_c^{air} values of sugi, pine, and the two poplar trees (Bernacchi et al. 2002). The K_c^{air} (μmol mol^{-1}) values of Bean_H, BPop_L, BPop_H, and Sugi_L were 455 at 26 °C, 659 at 26 °C, 601 at 25 °C and 722 at 27 °C, respectively; those of SPop_F, Sugi_F and Pine_F were all 722 at 27 °C (see Table 1 for these abbreviations).

Table 1 Abbreviations for the plant materials

	Scientific name	Common name	Growth condition	Plant group
GC-grown plants				
Bean_H	*Phaseolus vulgaris*	French bean	H	Angiosperm
BPop_L	*Populus nigra*	Black poplar	L	Angiosperm
BPop_H	*Populus nigra*	Black poplar	H	Angiosperm
Sugi_L	*Cryptomeria japonica*	Sugi, Japanese cedar	L	Conifer/Gymnosperm
Field-grown plants				
SPop_F	*Populus alba*	Silver poplar	F	Angiosperm
Sugi_F	*Cryptomeria japonica*	Sugi, Japanese cedar	F	Conifer/Gymnosperm
Pine_F	*Pinus densiflora*	Red pine	F	Conifer/Gymnosperm

Leaf samples for NH_3 gas exchange, GS activity and NH_3 leakiness measurements were obtained from the plants grown in an environmentally controlled growth chamber (GC-grown) and those grown under field conditions (Field-grown). H, cultivated under high-light and high-nutrient supply condition; L, cultivated under low-light and low-nutrient supply condition; F, cultivated in a tree garden of FFPRI

Leaf total GS activity

Total activity of leaf GS enzymes was measured according to the methods described by Vézina et al. (1988) and Lea et al. (1990). Leaf soluble protein extracts were incubated in a reaction buffer containing 100 mM HEPES-KOH (pH 7.8), 90 mM glutamate, 20 mM $MgSO_4$, 9 mM ATP, 6 mM hydroxylamine, and 1 mM EDTA. After 20 min of incubation at 30 °C, a stop solution containing 20% (v/v) trichloroacetic acid, 0.5 M $FeCl_3$, and 0.5 M HCl was added to the reaction mixture. The mixture was then centrifuged at 15,000 × *g* for 10 min to separate the supernatant. The absorbance of the supernatant was measured at 540 nm using a spectrophotometer (UV-1650PC; Shimadzu, Kyoto, Japan).

Statistical analyses

All statistical analyses were performed using SAS Add-In 6.1 for Microsoft office (SAS Institute, Cary, NC, USA).

Results

The absence of GS2 in Pinidae

Orthologues of GS in *Cryptomeria japonica* (sugi), a conifer in Cupressaceae, were searched in the EST database (FORESTGEN) based on the amino acid sequence of the Arabidopsis GS. We identified two types of *GS1* genes in sugi: *CjGS1a* and *CjGS1b* (Fig. S1). As was the case for a conifer in Pinaceae, *Pinus sylvestris* (Cantón et al. 1993), we did not obtain a *GS* gene containing an extended sequence, *GS2*.

We constructed a phylogenetic tree using the deduced amino acid sequences of *GS* genes from two angiosperm species (French bean and *Populus trichocarpa*) together with those from both conifers (Fig. 1a). The amino acid sequences of *CjGS1a* and *CjGS1b* from sugi were similar to those of *PsGS1a* and *PsGS1*b from *P. sylvestris*, respectively. The sequences of conifer GS1b (CjGS1b and PsGS1b) were structurally similar to those of angiosperm GS1 rather than those of conifer GS1a (CjGS1a and PsGS1a). This phylogenetic relationship was unchanged even when truncating the sequences of the GS2 transit peptides (Fig. S1) and analyzing the alignments (data not shown).

To confirm the results of phylogenetic analysis, we subjected leaf soluble proteins of *Populus alba* (silver poplar), *Populus nigra* (black poplar) and sugi to immunoblotting analysis using an anti-GS1 GS2 global antibody that cross-reacts with GS1 and GS2 derived from wide range of plant species (http://www.agrisera.com). Poplar (*P. trichocarpa*) possesses six GS1 (39.0–39.5 kDa) and two GS2 isoforms (42.2 kDa and 42.3 kDa) (Castro-Rodríguez et al. 2011;

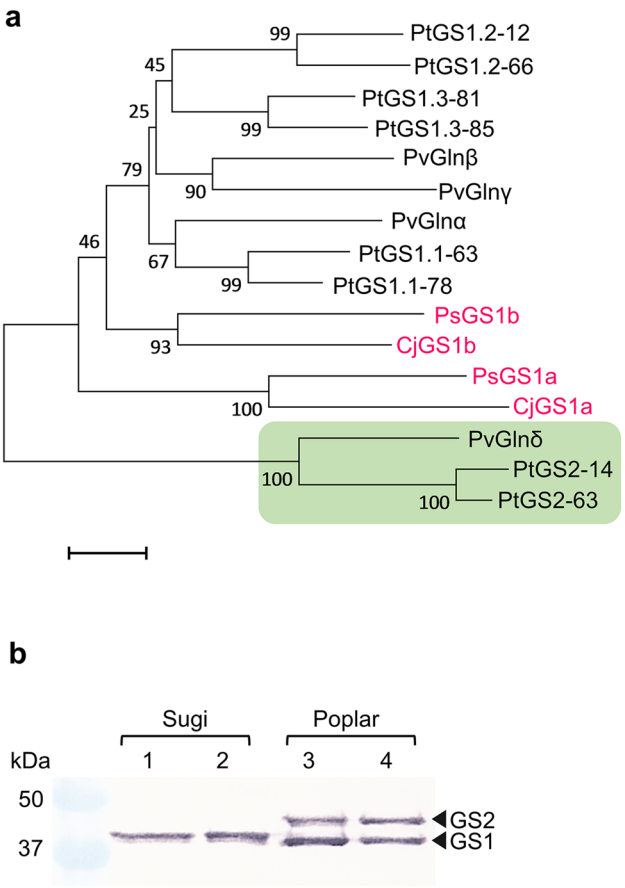

Fig. 1 **a** Phylogenetic tree constructed from alignments of the deduced amino acid sequences of *GS* genes from *Cryptomeria japonica* (sugi, Cj), *Populus trichocarpa* (poplar, Pt), *Phaseolus vulgaris* (French bean, Pv), and *Pinus sylvestris* (pine, Ps). Phylogenetic analysis of the full-length sequences was performed with the neighbor joining method. Bootstrap values are indicated at each branch point (1000 replicates). Bars correspond to two amino acid substitutions per 100 amino acid sites. Chloroplastic *GS* (*GS2*) are circled in green to be distinguished from the cytosolic form (*GS1*); conifer *GS* genes are in red. GenBank accession numbers are as follows: CjGS1a, LC331260; CjGS1b, LC331261; PtGS1.1-63, XP 002305885; PtGS1.1-78, XP 006372556; PtGS1.2-12, XP 002310666; PtGS1.2-66, XP 002306385; PtGS1.3-81, ABK94916; PtGS1.3-85, XP 002318305; PtGS2-14, XP 006380049; PtGS2-63, XP 002314425; PvGlnα, CAA27632; PvGlnβ, CAA27631; PvGlnγ, CAA32759; PvGlnδ, CAA31234; PsGS1a, CAA52448; PsGS1b, CAA06383. The names of the GS proteins for *P. trichocarpa* and those for *P. vulgaris* were assigned according to Castro-Rodríguez et al. (2011) and Lea (1997), respectively. **b** Immunoblotting analysis of leaf GS polypeptides from sugi, *Populus alba* (silver poplar) and *P. nigra* (black poplar). The Arabidopsis GS global antibody that recognizes both GS1 and GS2 was used. Molecular mass standards are shown on the left. 1, Field-grown sugi; 2, Growth chamber (GC)-grown sugi; 3, Field-grown silver poplar; 4, GC-grown black poplar

Fig. 1a). Two polypeptide bands that correspond to the GS1 and GS2 isoforms were detected in the leaves of black and silver poplars (Fig. 1b). By contrast, sugi leaves contained only a single band (Fig. 1b). The predicted molecular masses

of CjGS1a and CjGS1b from the amino acid sequence were 39.6 and 39.2 kDa, respectively. Our immunoblotting analysis is difficult to detect this 0.4 kDa difference between both isoforms. The single polypeptide band detected in sugi was therefore considered CjGS1a and/or CjGS1b.

We subjected seven angiosperm herbs and trees from seven different families and 13 coniferous species from six different families to immunoblotting analysis (Fig. 2). The leaves of all angiosperm species exhibited two clear GS1 and GS2 polypeptide bands except for French bean. Only GS2 band was clearly visible in the leaves of French bean whereas only GS1 band was obvious in the roots (Fig. 2). In French bean, identification of GS proteins through both ion exchange HPLC and immunoblotting analysis clarified that major abundance of GS2 in the bean leaves was responsible for the minor immunoblot GS1 band in their leaves (Cock et al. 1991). The opposite trend, namely, major abundance of GS1, was observed in the roots through ion exchange analysis (Lara et al. 1984). Our immunoblotting results were considered to support these previous findings. In all tested conifer leaves, a single polypeptide corresponding to GS1 was detected.

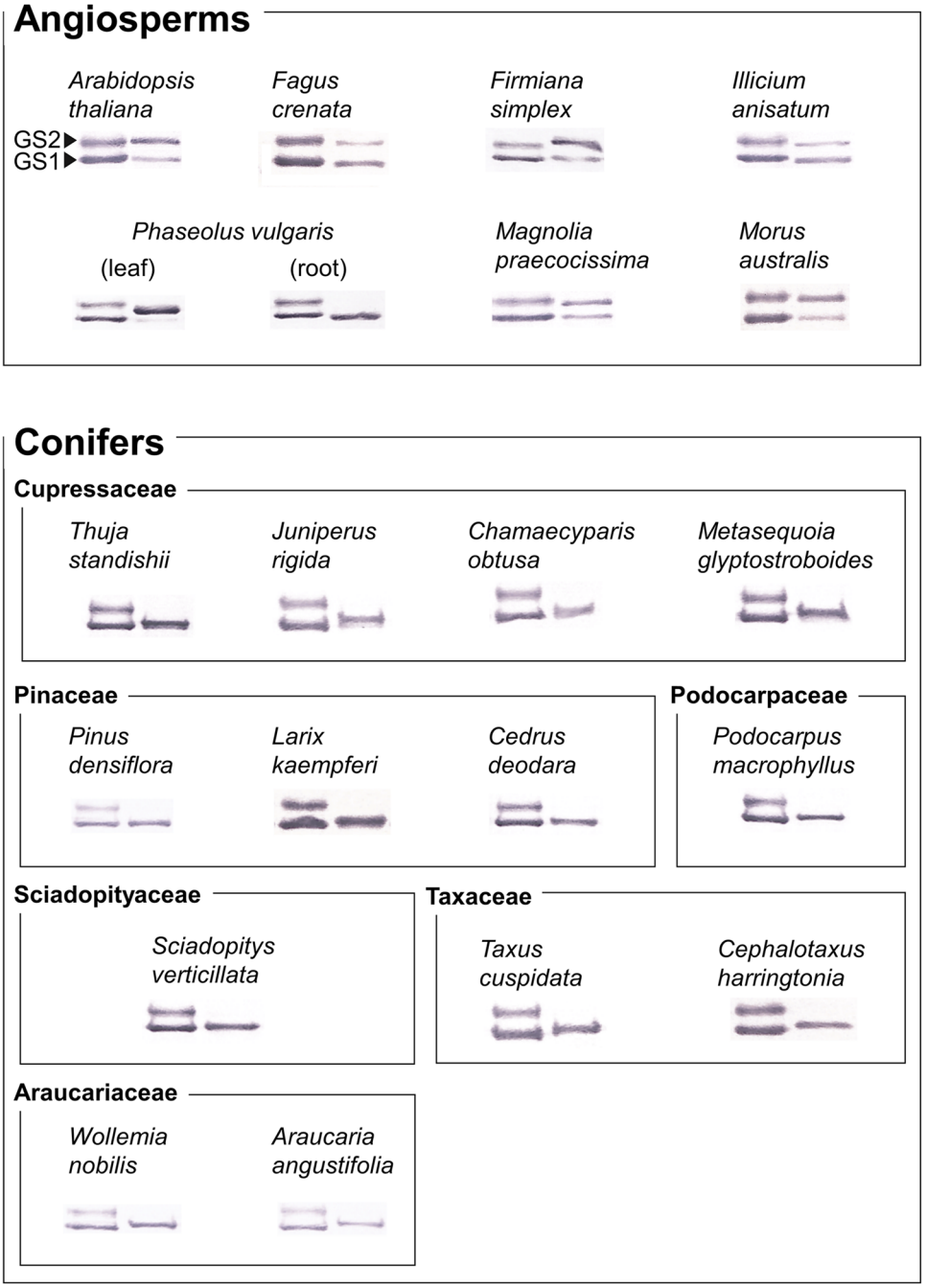

Fig. 2 Immunoblotting analysis of GS polypeptides from angiosperm and conifer leaves. Root samples were also analyzed for *Phaseolus vulgaris* (French bean). Soluble proteins (4 µg per lane) extracted from the samples were subjected to SDS–PAGE (right lane). Leaf soluble proteins from silver poplar were electrophoresed together as a positive control (left lane). The upper and lower bands from silver poplar correspond to the chloroplastic (GS2) and cytosolic (GS1) forms, respectively. Immunoblotting was performed with the Arabidopsis GS global antibody that recognizes both GS1and GS2

Table 2 Leaf CO_2/H_2O gas exchange and NH_3 gas exchange properties

	A^{area} (μmol m^{-2} s^{-1})	g_{tot}^{area} (mol m^{-2} s^{-1})	E^{area} (mmol m^{-2} s^{-1})	n_o (nmol mol^{-1})	n_e (nmol mol^{-1})	F_{NH3}^{area} (nmol m^{-2} s^{-1})	n
GC-grown plants							
Bean_H	19.4 ± 0.7a	0.57 ± 0.08a	3.95 ± 0.15a	4.4 ± 0.3a	2.84 ± 0.13a	−0.68 ± 0.14a	5
BPop_L	11.9 ± 0.5b	0.36 ± 0.08ab	4.0 ± 0.4a	5.07 ± 0.19a	2.59 ± 0.06a	−1.33 ± 0.16a	3
BPop_H	18.0 ± 1.0a	0.54 ± 0.09a	4.7 ± 0.3a	3.9 ± 0.7a	2.2 ± 0.6a	−1.4 ± 0.4a	6
Sugi_L	5.7 ± 1.0c	0.13 ± 0.04b	1.8 ± 0.4b	3.6 ± 0.4a	2.3 ± 0.5a	−1.36 ± 0.11a	4
Field-grown plants							
SPop_F	13.1 ± 0.9a	0.233 ± 0.015a	2.72 ± 0.07a	3.73 ± 0.11a	2.72 ± 0.19a	−0.49 ± 0.04a	8
Sugi_F	8.2 ± 1.5b	0.16 ± 0.02b	2.4 ± 0.3a	5.0 ± 0.4a	3.57 ± 0.18b	−2.2 ± 0.3b	7
Pine_F	17 ± 2a	0.21 ± 0.03a	4.4 ± 0.6b	4.5 ± 0.9a	3.0 ± 0.4ab	−4.3 ± 0.6c	4

We used plants grown in an environmentally controlled growth chamber (GC-grown) and those grown under field conditions (Field-grown). Abbreviations for the plant materials are shown in Table 1. A^{area}, net CO_2 fixation rate; g_{tot}^{area}, the total conductance (the conductance to water vapor diffusion through stomata and the boundary layer); E^{area}, transpiration rate; F_{NH3}^{area}, NH_3 absorption rate, all expressed per unit projected leaf area. n_o, and n_e are NH_3 mole fractions in the air leaving the gas exchange camber when containing leaves in the chamber and without leaves, respectively (Fig. 3). Data represent mean ± SE. n is the number of sample leaves. Different alphabets indicate significantly different means between GC- or field-grown species by Tukey–Kramer's post-hoc test at $P < 0.05$

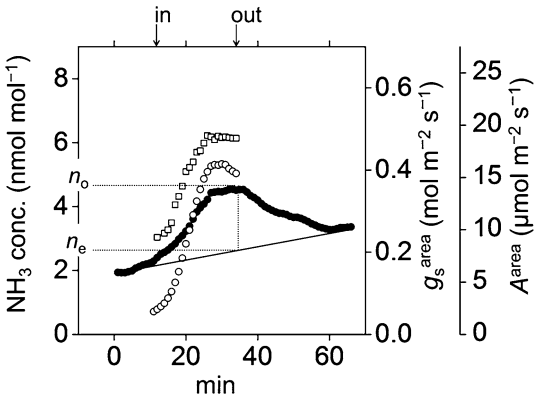

Fig. 3 Simultaneous measurements of NH_3 gas exchange and photosynthesis in a primary leaf of *Phaseolus vulgaris* (French bean). Time course of NH_3 mole fraction in air vented from the leaf chamber (solid circles), stomatal conductance to water vapor per unit leaf area (g_s^{area}, open circles), and net CO_2 fixation rate per unit leaf area (A^{area}, open squares). When g_s^{area} and A^{area} reached steady state, NH_3 mole fractions in the air (n_o and n_e) were obtained for the calculation of leaf NH_3 absorption rates using Eq. 2. For obtaining n_e values, the straight baselines were fitted by eye. Arrows on the x-axis indicate when the leaf was inside or outside the chamber

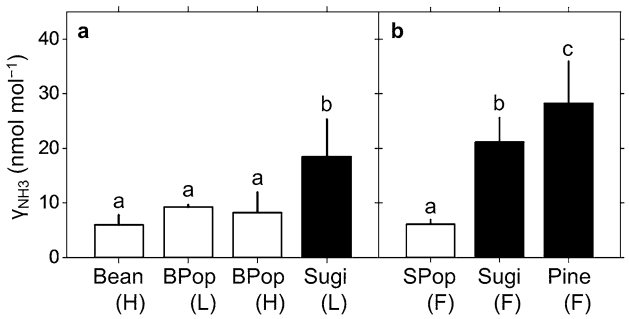

Fig. 4 Comparisons of leaf NH_3 compensation point (γ_{NH3}) between angiosperms (open bars) and conifers (solid bars). We used plants grown in an environmentally controlled growth chamber (**a** GC-grown) and those grown under field conditions (**b** Field-grown). Abbreviations for the plant materials are shown in Table 1. Data represent mean ± SD of 3–8 leaves. Different letters indicate significant differences of means between GC- or field-grown by Tukey–Kramer's post-hoc test at $P < 0.05$

High γ_{NH3} of conifer leaves

We measured the time courses of NH_3 emission from leaves under low ambient NH_3 concentration and used Eq. 1 to calculate NH_3 compensation point (γ_{NH3}) from the measured NH_3 gas exchange rates and the total conductance (Table 2). The results of French bean are shown in Fig. 3; NH_3 concentration in the air exhausted from the portable gas exchange chamber increased with the increases in stomatal conductance and net CO_2 assimilation rates. Similar results were found for all tested plants (data not shown). Farquhar et al. (1980a) already reported the γ_{NH3} of bean plants; the calculated γ_{NH3} of bean in our study was close to the value reported by Farquhar et al.

For the GC-grown plants, we found that the calculated γ_{NH3} of sugi grown under L-condition (Sugi_L) was significantly higher than that of black poplar and bean plants grown under H-condition (BPop_H and Bean_H, respectively) (Fig. 4a). We did not raise sugi plants under H-condition for measurements because a yellowing symptom appears in sugi leaves under this condition (see Materials and methods). Therefore, the different γ_{NH3} exhibited by these three species might result from differences in growth conditions. To check this possibility, we cultivated black poplar plants under L-condition (BPop_L) and compared their γ_{NH3} values. We found that the γ_{NH3} of BPop_L was similar to that

of BPop_H (Fig. 4a). The γ_{NH3} of Sugi_L was about twice higher than that of BPop_L, as was the case for the relationship between Sugi_L and BPop_H. Thus, growth conditions had negligible contributions to the high γ_{NH3} of sugi.

We also measured γ_{NH3} of leaves taken from the adult trees cultivated under a field (F) condition: silver poplar (SPop_F), sugi (Sugi_F) and pine (Pine_F) trees (Fig. 4b). The γ_{NH3} of Sugi_F was almost equal to that of the GC-grown sugi or Sugi_L (*t*-tests; $P = 0.44$). We found that the γ_{NH3} values of Sugi_F and Pine_F were significantly higher than that of SPop_F (Fig. 4b).

Relationships of NH_3 leakiness and leaf total GS activity to γ_{NH3}

To examine whether the higher γ_{NH3} of conifers (Fig. 4) is due to higher levels of unassimilated NH_3 from the photorespiration pathway, we measured changes in leaf NH_4^+ content in response to Rubisco oxygenation rate (v_o). We calculated v_o on the basis of the measured leaf CO_2 gas exchange rates under different CO_2 concentrations in a portable gas exchange chamber (Table 3).

The v_o of all studied plants increased when CO_2 concentration decreased from 800 to 100 ppm. Except for BPop_L and SPop_F, the leaf NH_4^+ content of all species significantly increased with the v_o increases (Fig. 5). We also measured the leaf NH_4^+ content under dark condition at 400 ppm CO_2 (Fig. 5a). The leaf NH_4^+ content of Sugi_L was larger than that of other three plants (BPop_H, BPop_L and and Bean_H plants) under dark treatment.

The increase in leaf NH_4^+ content per unit v_o increment, i.e. the slope of the linear relationship between the NH_4^+ content and v_o (Fig. 5), can be used as an index of the amount of unassimilated NH_3 directly produced from the photorespiration pathway. We defined the amount of unassimilated NH_3 divided by a CO_2 treatment period as "NH_3 leakiness" (see Eq. 3). We calculated the NH_3 leakiness of each species and found that NH_3 leakiness had a significant positive correlation with the γ_{NH3} (Fig. 6a). By

Table 3 Leaf photosynthesis parameters for calculating Rubisco oxygenation rate (v_o) and leaf chlorophyll (Chl) content

	$[CO_2]$ (ppm)	Bean_H	BPop_L	BPop_H	Sugi_L
GC-grown plants					
A (μmol mmol Chl^{-1} s^{-1})	100	8.8 ± 0.4 (3)	6.7 ± 1.7 (3)	10.0 ± 0.8 (11)	1.00 ± 0.18 (14)
	200	ND	ND	27 ± 3 (11)	3.4 ± 0.2 (9)
	400	ND	ND	48 ± 2 (13)	7.3 ± 0.8 (11)
	800	57 ± 3 (3)	55 ± 4 (3)	55 ± 2 (7)	13.1 ± 1.2 (8)
C_i (μmol mol^{-1})	100	88 ± 2 (3)	90.5 ± 0.5 (3)	90.8 ± 1.5 (11)	87.9 ± 1.6 (14)
	200	ND	ND	176.5 ± 3.3 (11)	166 ± 2 (9)
	400	ND	ND	358.3 ± 1.6 (13)	309 ± 7 (11)
	800	693 ± 16 (3)	658 ± 48 (3)	721 ± 6 (7)	586 ± 18 (8)
R_{dark} (μmol mmol Chl^{-1} s^{-1})	400	2.7 ± 0.4 (3)	3.2 ± 0.3 (3)	2.38 ± 0.14 (3)	2.2 ± 0.4 (4)
g_m (mol mmol Chl^{-1} s^{-1})	NA	0.9 ± 0.3 (3)	0.94 ± 0.05 (3)	1.2 ± 0.3 (3)	0.096 ± 0.009 (3)
Chl content (mmol m^{-2})	NA	0.51 ± 0.03 (6)	0.332 ± 0.03 (6)	0.52 ± 0.03 (8)	1.33 ± 0.15 (10)
	$[CO_2]$ (ppm)	SPop_F	Sugi_F	Pine_F	
Field-grown plants					
A (μmol mmol Chl^{-1} s^{-1})	100	3.1 ± 0.4 (4)	1.45 ± 0.19 (5)	1.63 ± 0.14 (4)	
	800	28 ± 5 (4)	17.2 ± 1.7 (5)	16.8 ± 0.3 (5)	
C_i (μmol mol^{-1})	100	89.7 ± 1.0 (4)	83.2 ± 1.2 (5)	83.2 ± 0.8 (4)	
	800	602 ± 11 (4)	559 ± 29 (5)	601 ± 9 (5)	
R_{dark} (μmol mmol Chl^{-1} s^{-1})	400	1.56 ± 0.15 (3)	1.6 ± 0.2 (3)	0.80 ± 0.10 (3)	
g_m (mol mmol Chl^{-1} s^{-1})	NA	0.62 ± 0.17 (3)	0.44 ± 0.18 (3)	0.7 ± 0.2 (3)	
Chl content (mmol m^{-2})	NA	0.53 ± 0.02 (6)	1.33 ± 0.12 (6)	1.27 ± 0.10 (6)	

We used plants grown in an environmentally controlled growth chamber (GC-grown) and those grown under field conditions (Field-grown). Abbreviations for the plant materials are shown in Table 1. $[CO_2]$ denotes the CO_2 concentration in the portable gas exchange chamber. A, net CO_2 fixation rate; C_i, the intercellular CO_2 concentration; R_{dark}, dark respiration rate; g_m, mesophyll conductance to CO_2 diffusion, all these parameters are expressed per unit leaf chlorophyll content except for C_i. Chl content are expressed per unit projected leaf area. g_m was estimated through the A–C_i curve fitting method (Ethier and Livingston 2004; Fig. S2). Data represent mean ± SE. Values in parentheses indicate the number of sample leaves

NA, not applicable; ND, not determined

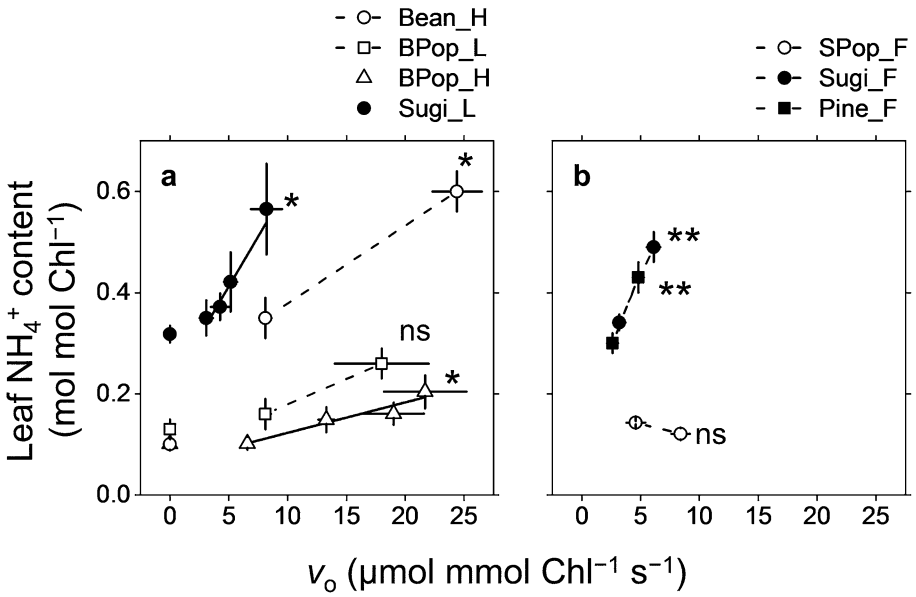

Fig. 5 Relationship between leaf NH_4^+ content and Rubisco oxygenation rate (v_o) in angiosperms (open symbols) and conifers (solid symbols). Leaf NH_4^+ content and v_o are both expressed per unit chlorophyll content. We used plants grown in an environmentally controlled growth chamber (**a** GC-grown) and those grown under field conditions (**b** Field-grown). Abbreviations for the plant materials are shown in Table 1. Illuminated leaves were subjected to different CO_2 concentrations ranging from 100 to 800 ppm (CO_2 treatment) for one hour. For the GC-grown plants, we also plotted the data for leaves subjected to dark treatment. v_o was estimated from the gas exchange data (Table 3) while it assumed to be zero for dark treatment. There were significant linear relationships using the data excluded for dark treatment (solid lines; $P<0.05$). *t*-tests were conducted on the NH_4^+ content between the 100 and 800 ppm CO_2 treatments (*$P<0.05$, **$P<0.01$, ns, not significant). Data represent mean ± SE. The number of sample leaves (*n*) are shown in Table 3 for CO_2 treatment. *n* was 3 or 5 for dark treatment

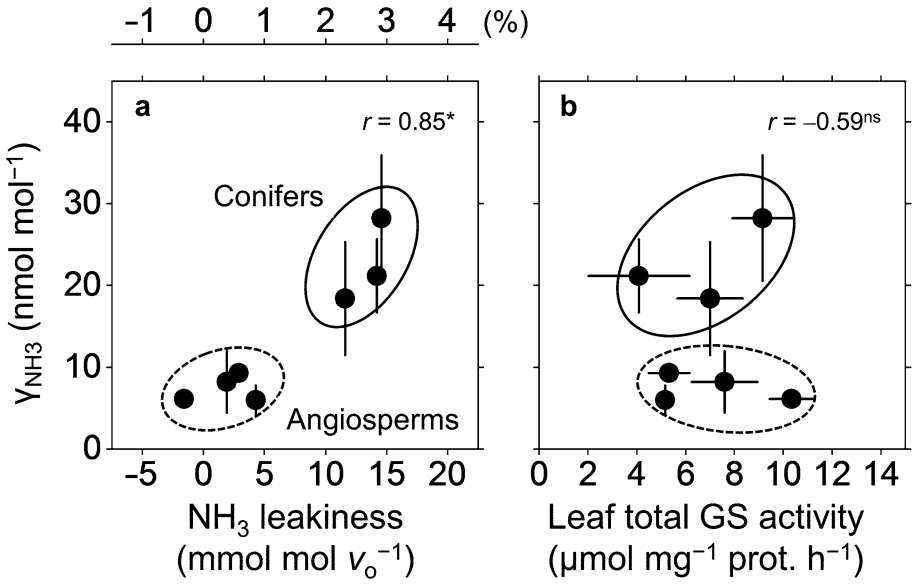

Fig. 6 Relationships of NH_3 leakiness (**a**) and leaf total GS activity (**b**) to leaf NH_3 compensation point (γ_{NH3}). NH_3 leakiness was calculated from both slope of the linear function of Rubisco oxygenation rate (v_o) to leaf NH_4^+ content in Fig. 5 and a CO_2 treatment period. The symbols circled in solid and dashed lines represent the conifer and angiosperm species used in this study, respectively. The total GS activity is expressed per unit soluble protein content. The scale above the left panel corresponds to a percentage of unassimilated (i.e. leaked) NH_3 produced from the photorespiration pathway according to the FvCB model (Farquhar et al. 1980b). Regression coefficients (*r*) are shown (*$P<0.05$; ns, not significant). γ_{NH3} and GS activity data represent mean ± SD of 3–8 leaves

contrast, the differences in γ_{NH3} were not related with the leaf total GS activities between species (Fig. 6b).

Based on the FvCB model, 0.5 molecule of NH_3 is produced per mol v_o (Farquhar et al. 1980b). Using this model, we estimated that nearly 3% of NH_3 produced per v_o was unassimilated (i.e. leaked) in conifers such as sugi and pine (Figs. 6a, 7). On the other hand, in angiosperms such as bean and poplar, only less than 1% of NH_3 was leaked.

Discussion

Low assimilation efficiency of photorespiratory NH_3 in conifers that lack GS2

Genetic information and immunoblotting analyses revealed that GS1, but not GS2, is present in sugi (*Cryptomeria japonica*), a member of the family Cupressaceae (Fig. 1). This is the first report showing that a non-Pinacease conifer also lacks GS2. Although the absence of GS2 needs further checking by immunolocalization analysis at the electron microscopy level as was the case for the study in *Pinus pinaster* (García-Gutiérrez et al. 1998), our immunoblotting analyses clearly indicated that leaves from coniferous species from all family members in Pinidae exhibited only GS1 band (Fig. 2). Thus, our results suggest that the absence of GS2 is common in conifers.

NH_3 produced from the photorespiration pathway is assimilated by GS2 in angiosperms. In conifers, one of the GS1 isoforms, GS1a, is a potential isoform that might fulfill the GS2 function (Avila et al. 2001; Suárez et al. 2002) (Fig. 7). The cysteine residues of the GS2 sequences are involved in the redox regulation of this enzyme and these residues are not observed in angiosperm GS1 (Choi et al. 1999). It is noteworthy that the conifer GS1a sequences, but not the GS1b, possess one of the cysteine residues (Fig. S1). This could be an evidence that conifer GS1a has an orthologous function to GS2.

The FvCB model estimated that nearly 3% of NH_3 produced per v_o was unassimilated (i.e. leaked) in conifers whereas only less than 1% of the NH_3 was leaked in angiosperms (Figs. 6a, 7). Higher NH_3 leakiness, thereby lower assimilation efficiency of photorespiratory NH_3, could be disadvantage for conifers due to high photorespiration activity under the present levels of atmospheric CO_2 and O_2.

Sensitivity of NH_3 leakiness to g_m and Γ*

As inferred from Eqs. 3–6, NH_3 leakiness depends on the estimated g_m and Γ* values. Several methods, such as chlorophyll fluorescence method, stable isotope method, and curve-fitting method, have been developed for g_m estimation (Epron et al. 1995; Ethier and Livingston 2004; von Caemmerer and Evans 1991). The g_m values estimated through

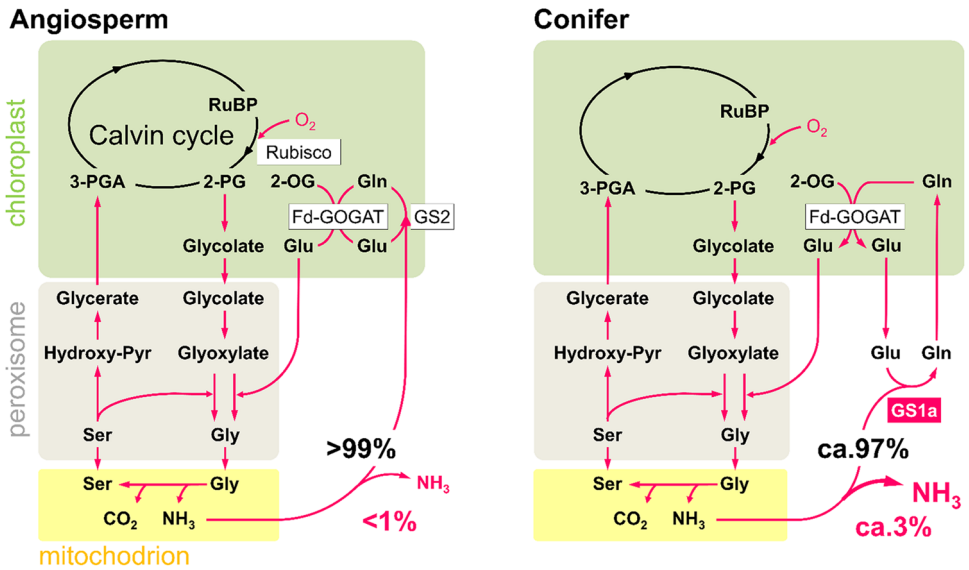

Fig. 7 Comparison of photorespiration pathways between angiosperms and conifers. The conifer photorespiration pathway is based on the pathway provided by Suárez et al. (2002). Photorespiration starts with the oxygenation of ribulose-1,5-bisphosphate (RuBP) by Rubisco. Hydroxy-Pyr, hydroxypyruvate; Gln, glutamine; Glu, glutamate; Gly, glycine; 2-OG, 2-oxoglutarate; 2-PG, 2-phosphoglycolate; 3-PGA, 3-phosphoglycerate; Ser, serine. Less than 1% and nearly 3% of the photorespiratory-produced NH_3 from the mitochondria is estimated to be leaked in angiosperms and conifers, respectively (Fig. 6). GS located in chloroplasts (GS2) and ferredoxin-glutamate synthase (Fd-GOGAT) are involved in assimilation of photorespiratory NH_3 in angiosperms. The cytosolic GS1a and the chloroplastic Fd-GOGAT are the candidate enzymes involved in assimilation of photorespiratory NH_3 in conifers (Suárez et al. 2002)

the curve-fitting method are almost in good agreement with those estimated with the chlorophyll fluorescence method in tobacco (Miyazawa et al. 2008) and in gymnosperms including conifers (Veromann-Jürgenson et al. 2017). There was a significant positive relationship between the g_m and the light-saturate rates of net CO_2 fixation at ambient CO_2 in our study ($P < 0.05$; Fig. S3). As compared with those relationships reported in literature, our estimated g_m values were considered to be relevant. The simultaneous application of more than two methods is, however, recommended for precise g_m estimation (Pons et al. 2009). We then performed a sensitivity analysis to identify to what extent changes in g_m affect NH_3 leakiness, and found that NH_3 leakiness was almost unaffected by changes in g_m (Fig. S4).

As in Eq. 5, the Γ* is determined by $S_{c/o}$. The $S_{c/o}$ of bean plants is available from the literature (Hermida-Carrera et al. 2016), whereas those of poplar, sugi, and pine are unknown. We performed a sensitivity analysis to determine to what extent the uncertainty of Γ* affects NH_3 leakiness (Fig. S4). We calculated Γ* range on the basis of the reported $S_{c/o}$ values of purified Rubisco from 28 species of C3 crops and trees (Galmés et al. 2005; Hermida-Carrera et al. 2016). We found that the NH_3 leakiness values of sugi and pine trees were always higher than those of bean and poplar within this Γ* range (Fig. S4). Taken together, NH_3 leakiness was robust to changes in estimated g_m and Γ* values.

Comparison with γ_{NH3} values reported in literature

The values of γ_{NH3} have been intensively studied in crops and grasses such as barley, bromegrass, French bean, oilseed rape, perennial ryegrass, and rice; γ_{NH3} ranges from 0.1 to 10 nmol mol^{-1} under ambient temperatures (Farquhar et al. 1980a; Hayashi et al. 2008; Miyazawa et al. 2014; Wang et al. 2013). The γ_{NH3} is affected by the availability of soil nitrogen because NH_4^+ and/or NO_3^- are transported to leaves *via* the transpiration stream from soils (Hayashi et al. 2008; Husted et al. 2000). For example, bromegrass cultivated on medium with extremely high nitrogen content has a γ_{NH3} value of approximately 10 nmol mol^{-1} (6 mM NH_4HCO_3 in medium) (Mattsson and Schjoerring 2002). In our study, GC-sugi saplings were raised on a medium with moderate nitrogen content (0.9 mM NH_4NO_3), suggesting that the high γ_{NH3} of sugi (18.4 nmol mol^{-1} on average at 27 °C) cannot be attributed to high soil nitrogen.

There are only a few reports on the γ_{NH3} of trees, particularly those of conifers. The γ_{NH3} of mature green leaves from field-grown *Fagus sylvatica*, a deciduous broad-leaved tree, was 3 nmol mol^{-1} at 25 °C; this γ_{NH3} value is similar to those reported for crops and grasses (Wang et al. 2011). Geßler et al. (2002) studied changes in the F_{NH3} of twigs from adult conifers (spruce) fumigated with various concentrations of NH_3 (2.4 to 135 nmol mol^{-1}) under field conditions of fluctuating light and air temperature. They estimated the γ_{NH3} of spruce by conducting linear regression between F_{NH3} and air-NH_3 concentration. They found that the γ_{NH3} of spruce was approximately 2.5 nmol mol^{-1}, which was lower than those of sugi and pine trees in our study and close to that of crops and grasses. Geßler et al. (2002) measured the F_{NH3} of spruce twigs exposed to low light intensities under which photorespiration rates are reduced (< 200 μmol m^{-2} s^{-1} for most measurement data in Geßler et al. *vs*. 800 μmol m^{-2} s^{-1} in our study). Low photorespiration activity decreases the γ_{NH3} in barley (Wang et al. 2013). The different light conditions in the study of Geßler et al. from that in our study might explain this inconsistency.

Is acquisition of GS2 as an adaptive mechanism to low CO_2 environments on earth?

Cánovas et al. (2007) speculated that the acquisition of GS2 is an adaptive mechanism to high levels of photorespiratory NH_3 when plants encountered the present oxygen levels in the atmosphere during land plant evolution. Our present study is the first report demonstrating that assimilation efficiency of photorespiratory NH_3 differs between angiosperms and conifers that lack GS2 (Fig. 6).

Gymnosperm consists of four groups: Cycadidae, Ginkgoidae, Gnetidae and Pinidae (Christenhusz et al. 2011). García-Gutiérrez et al. (1998) found that leaves of a gymnosperm, *Ginkgo biloba* (Ginkgoidae), exhibited GS1 and GS2 polypeptide bands by immunoblotting analysis. This result was confirmed by our analysis in *Ginkgo* (Fig. S5). We subjected leaves of some species from the other two gymnosperm groups such as *Cycas revoluta* (Cycadidae), *Ephedra minima* (Gnetidae), *Gnetum gnemon* (Gnetidae) and *Welwitschia mirabilis* (Gnetidae) to immunoblotting, and found that all these gymnosperm species exhibited only GS1 band (Fig. S5). Therefore, except for *Ginkgo*, the absence of GS2 appears to be common in gymnosperms.

Angiosperms are presently the most dominant plant group on earth while gymnosperms were the dominant group during the Triassic and Jurassic periods (250 – 145 Mys ago) (Haworth et al. 2011). Atmospheric CO_2 level was higher than the present average level of 400 ppm and likely fluctuated between 1200 and 1800 ppm during these periods (Haworth et al. 2011; Sage 2013). On the other hand, the estimated atmospheric O_2 levels ranged from 15 to 20%, which was similar to the present level (Berner 1999; Haworth et al. 2011). Such high CO_2 environment would have suppressed the NH_3 production because of low photorespiration activity. In this context, the disadvantage of absence of GS2 might not have been crucial for gymnosperms under such high CO_2 environments on earth. To get a clearer picture of the evolutionary significance of GS2,

further studies need to confirm whether GS2 is absent from the early divergent lineage including ferns and mosses.

How does GS2 contribute to efficient assimilation of photorespiratory NH_3?

Analyses of purified poplar GS2 and recombinant *Pinus* GS1a (PsGS1a) enzymes from previous studies indicated that K_m or $S_{0.5}$ values for the NH_4^+, glutamate and ATP were lower or similar in PsGS1a than those in poplar GS2 (de la Torre et al. 2002; Fu et al. 2003). This means that the differences in the substrate affinities between both GS enzymes fail to explain the lower assimilation efficiency of photorespiratory NH_3 in conifers. Glutamate is known to be enriched in the chloroplasts (Mills and Joy 1980). It is tempting to speculate that subcellular differences in the substrate concentrations for GS such as the glutamate concentration can explain the difference in the assimilation efficiency between conifers and angiosperms.

Acknowledgements We thank Dr. Mitsutoshi Kitao, Dr. Hiroyuki Tobita, and Dr. Satoru Takanashi in FFPRI for providing support for gas exchange measurements. We also thank Dr. Tokuko Ihara-Udino in FFPRI for her help searching the EST database, Dr. Tomohiro Igasaki and Ms. Ai Hagiwara in FFPRI for their help growing plant materials, and Dr. Eiichi Minami and Dr. Masao Iwamoto in National Agriculture and Food Research Organization (Tsukuba, Japan) for the use of HPLC. We used SAS software provided by AFFRIT, MAFF, Japan. This work was supported by JSPS KAKENHI Grant No. 16K07791 and Research grant #201705 of FFPRI. S-IM thanks anonymous reviewers for constructive comments on early drafts of the manuscript.

References

Avila C, García-Gutiérrez A, Crespillo R, Cánovas FM (1998) Effects of phosphinotricin treatment on glutamine synthetase isoforms in Scots pine seedlings. Plant Physiol Biochem 36:857–863

Avila C, Suárez MF, Gómez-Maldonado J, Cánovas FM (2001) Spatial and temporal expression of two cytosolic glutamine synthetase genes in Scots pine: functional implications on nitrogen metabolism during early stages of conifer development. Plant J 25:93–102

Avila-Sáez C, Muñoz-Chapuli R, Plomion C, Frigerio J-M, Cánovas FM (2000) Two genes encoding distinct cytosolic glutamine synthetases are closely linked in the pine genome. FEBS lett 477:237–243

Bauer D, Biehler K, Fock H, Carrayol E, Hirel B, Migge A, Becker TW (1997) A role for cytosolic glutamine synthetase in the remobilization of leaf nitrogen during water stress in tomato. Physiol Plant 99:241–248

Bernacchi CJ, Portis AR, Nakano H, von Caemmerer S, Long SP (2002) Temperature response of mesophyll conductance. Implications for the determination of rubisco enzyme kinetics and for limitations to photosynthesis in vivo. Plant Physiol 130:1992–1998

Berner RA (1999) Atmospheric oxygen over Phanerozoic time. Proc Natl Acad Sci USA 96:10955–10957

Blackwell RD, Murray AJS, Lea PJ (1987) Inhibition of photosynthesis in barley with decreased levels of chloroplastic glutamine synthetase activity. J Exp Bot 38:1799–1809

Cánovas FM, Cantón FR, Gallardo F, García-Gutiérrez A, de Vicente A (1991) Accumulation of glutamine synthetase during early development of maritime pine (*Pinus pinaster*) seedlings. Planta 185:372–378

Cánovas FM, Avila C, Cantón FR, Cañas RA, de la Torre F (2007) Ammonium assimilation and amino acid metabolism in conifers. J Exp Bot 58:2307–2318

Cantón FR, García-Gutiérrez A, Gallardo F, de Vicente A, Cánovas FM (1993) Molecular characterization of a cDNA clone encoding glutamine synthetase from a gymnosperm, *Pinus sylvestris*. Plant Mol Biol 22:819–828

Castro-Rodríguez V, García-Gutiérrez A, Canales J, Avila C, Kirby EG, Cánovas FM (2011) The glutamine synthetase gene family in *Populus*. BMC Plant Biol 11:119

Choi YA, Kim SG, Kwon YM (1999) The plastidic glutamine synthetase activity is directly modulated by means of redox change at two unique cysteine residues. Plant Sci 149:175–182

Christenhusz MJM, Reveal JL, Farjon A, Gardner MF, Mill RR, Chase MW (2011) A new classification and linear sequence of extant gymnosperms. Phytotaxa 19:55–70

Cock JM, Brock IW, Watson AT, Swarup R, Morby AP, Cullimore JV (1991) Regulation of glutamine synthetase genes in leaves of *Phaseolus vulgaris*. Plant Mol Biol 17:761–771

de la Torre F, García-Gutiérrez A, Crespillo R, Cantón F, Ávila C, Cánovas FM (2002) Functional expression of two pine glutamine synthetase in bacteria reveals that they encode cytosolic holoenzymes with different molecular and catalytic properties. Plant Cell Physiol 43:802–809

Epron D, Godard D, Cornic G, Genty B (1995) Limitation of net CO_2 assimilation rate by internal resistances to CO_2 transfer in the leaves of two tree species (*Fagus sylvatica* L.nd *Castanea sativa* Mill.). Plant Cell Environ 18:43–51

Ethier GJ, Livingston NJ (2004) On the need to incorporate sensitivity to CO_2 transfer conductance into the Farquhar–von Caemmerer–Berry leaf photosynthesis model. Plant Cell Environ 27:137–153

Farquhar GD, Firth PM, Wetselaar R, Weir B (1980a) On the gaseous exchange of ammonia between leaves and the environment: determination of the ammonia compensation point. Plant Physiol 66:710–714

Farquhar GD, von Caemmerer S, Berry JA (1980b) A biochemical model of photosynthetic CO_2 assimilation in leaves of C3 species. Planta 149:78–90

Fu J, Sampalo R, Gallardo F, Cánovas FM, Kirby EG (2003) Assembly of a cytosolic pine glutamine synthetase holoenzyme in leaves of transgenic poplar leads to enhanced vegetative growth in young plants. Plant Cell Environ 26:411–418

Galmés J, Flexas J, Keys AJ, Cifre J, Mitchell RAC, Madgwick PJ, Haslam RP, Medrano H, Parry MAJ (2005) Rubisco specificity factor tends to be larger in plant species from drier habitats and in species with persistent leaves. Plant Cell Environ 28:571–579

García-Gutiérrez A, Dubois F, Cantón FR, Gallardo F, Sangwan RS, Cánovas FM (1998) Two different modes of early development and nitrogen assimilation in gymnosperm seedlings. Plant J 13:187–199

Geßler A, Rienks M, Rennenberg H (2002) Stomatal uptake and cuticular adsorption contribute to dry deposition of NH_3 and NO_2 to needles of adult spruce (*Picea abies*) trees. New Phytol 156:179–194

Haworth M, Elliot-Kingston C, McElwain JC (2011) Stomatal control as a driver of plant evolution. J Exp Bot 62:2419–2423

Hayashi K, Hiradate S, Ishikawa S, Nouchi I (2008) Ammonia exchange between rice leaf blade and the atmosphere: Effect of broadcast urea and changes in xylem sap and leaf apoplastic ammonium concentrations. Soil Sci Plant Nutr 54:807–818

Hermida-Carrera C, Kapralov MV, Galmés J (2016) Rubisco catalytic properties and temperature response in crops. Plant Physiol 171:2549–2561

Husted S, Hebbern CA, Mattsson M, Schjoerring JK (2000) A critical experimental evaluation of methods for determination of NH_4^+ in plant tissue, xylem sap and apoplastic fluid. Physiol Plant 109:167–179

Kamachi K, Yamaya T, Hayakawa T, Mae T, Ojima K (1992) Vascular bundle-specific localization of cytosolic glutamine synthetase in rice leaves. Plant Physiol 99:1481–1486

Kozaki A, Takeba G (1996) Photorespiration protects C3 plants from photooxidation. Nature 384:557–560

Kumagai E, Araki T, Hamaoka N, Ueno O (2011) Ammonia emission from rice leaves in relation to photorespiration and genotypic differences in glutamine synthetase activity. Ann Bot 108:1381–1386

Lara M, Porta H, Padilla J, Folch J, Sánchez F (1984) Heterogeneity of glutamine synthetase polypeptides in *Phaseolus vulgaris* L. Plant Physiol 76:1019–1023

Lea PJ (1997) Primary nitrogen metabolism. In: Dey PM, Harborne JB (eds) Plant biochemistry. Academic Press, London, pp 273–313

Lea PJ, Blackwell RD, Chen F-L, Hecht U (1990) Enzymes of ammonia assimilation. In: Lea PJ (ed) Methods in plant biochemistry, vol 3. Academic Press, London, pp 257–276

Lightfoot DA, Green NK, Cullimore JV (1988) The chloroplast-located glutamine synthetase of *Phaseolus vulgaris* L.: nucleotide sequence, expression in different organs and uptake into isolated chloroplasts. Plant Mol Biol 11:191–202

Mattsson M, Schjoerring JK (2002) Dynamic and steady-state responses of inorganic nitrogen pools and NH_3 exchange in leaves of *Lolium perenne* and *Bromus erectus* to changes in root nitrogen supply. Plant Physiol 128:742–750

Mills WR, Joy KW (1980) A rapid method for isolation of purified, physiologically active chloroplasts, used to study the intracellular distribution of amino acids in pea leaves. Planta 148:75–83

Miyazawa S-I, Yoshimura S, Shinzaki Y, Maeshima M, Miyake C (2008) Deactivation of aquaporins decreases internal conductance to CO_2 diffusion in tobacco leaves grown under long-term drought. Funct Plant Biol 35:553–564

Miyazawa S-I, Hayashi K, Nakamura H, Hasegawa T, Miyao M (2014) Elevated CO_2 decreases the photorespiratory NH_3 production but does not decrease the NH_3 compensation point in rice leaves. Plant Cell Physiol 55:1582–1591

Pons TL, Flexas J, von Caemmerer S, Evans JR, Genty B, Ribas-Carbo M, Brugnoli E (2009) Estimating mesophyll conductance to CO_2: methodology, potential errors, and recommendations. J Exp Bot 60:2217–2234

Porra RJ, Thompson WA, Kriedemann PE (1989) Determination of accurate extinction coefficients and simultaneous equations for assaying chlorophylls *a* and chlorophyll *b* extracted with four different solvents: verification of the concentration of chlorophyll standards by atomic absorption spectroscopy. Biochim Biophys Acta 975:384–394

Razal RA, Ellis S, Singh S, Lewis NG, Towers GHN (1996) Nitrogen recycling in pheylpropanoid metabolism. Phytochem 41:31–35

Sage RF (2013) Photorespiratory compensation: a driver for biological diversity. Plant Biol 15:624–638

Sakurai N, Hayakawa T, Nakamura T, Yamaya T (1996) Changes in the cellular localization of cytosolic glutamine synthetase protein in vascular bundles of rice leaves at various stages of development. Planta 200:306–311

Somerville CR, Ogren WL (1980) Inhibition of photosynthesis in *Arabidopsis* mutants lacking leaf glutamate synthase activity. Nature 286:257–259

Suárez MF, Avila C, Gallardo F, Cantón FR, García-Gutiérrez A, Claros MG, Cánovas FM (2002) Molecular and enzymatic analysis of ammonium assimilation in woody plants. J Exp Bot 53:891–904

Tamura K, Stecher G, Peterson D, Filipski A, Kumar S (2013) MEGA6: Molecular Evolutionary Genetics Analysis version 6.0. Mol Biol Evol 30:2725–2729

Tsuchida H, Tamai T, Fukayama H, Agarie S, Nomura M, Onodera H, Ono K, Nishizawa Y, Lee B-H, Hirose S, Toki S, Ku MSB, Matsuoka M, Miyao M (2001) High level expression of C_4-specific NADP-malic enzyme in leaves and impairment of photoautotrophic growth of a C_3 plant, rice. Plant Cell Physiol 42:138–145

Veromann-Jürgenson L-L, Tosens T, Laanisto L, Niinemets Ü (2017) Extremely thick cell walls and low mesophyll conductance: welcome to the world of ancient living! J Exp Bot 68:1639–1653

Vézina L-P, Margolis HA, Ouimet R (1988) The activity, characterization and distribution of the nitrogen assimilation enzyme, glutamine synthetase, in jack pine seedlings. Tree Physiol 4:109–118

von Caemmerer S, Evans JR (1991) Determination of the average partial pressure of CO_2 in chloroplasts from leaves of several C3 plants. Aust J Plant Physiol 18:287–305

Wallsgrove RM, Turner JC, Hall NP, Kendall AC, Bright SWJ (1987) Barley mutants lacking chloroplast glutamine synthetase—biochemical and genetic analysis. Plant Physiol 83:155–158

Wang L, Xu Y, Schjoerring JK (2011) Seasonal variation in ammonia compensation point and nitrogen pools in beech leaves (*Fagus sylvatica*). Plant Soil 343:51–66

Wang L, Pedas P, Eriksson D, Schjoerring JK (2013) Elevated atmospheric CO_2 decreases the ammonia compensation point of barley plants. J Exp Bot 64:2713–2724